

# Modeling of direct and inverse problems in light scattering by rough surfaces

CZESŁAW ŁUKIANOWICZ

Mechanical Department, Technical University of Koszalin,  
ul. Raclawicka 15–17, 75–620 Koszalin, Poland, e-mail: czel@tu.koszalin.pl.

The rough surface assessment by light scattering methods is mostly preceded by the solution to the so-called direct and inverse problem. It requires assuming the mutual theoretical model, describing the phenomenon of light scattering by rough surfaces, for both problems. In general, despite application of numerous simplifications, it is an intricate diffraction model. The description of the rough surface geometry is also quite often complicated. Therefore, in many cases experimental verification of analytical solutions to the direct and inverse problems is very difficult. Under such circumstances it is advisable to verify the correctness of the solutions obtained using the computer-modeling methods. The paper presents the process of the direct and inverse problem modeling and covers the results of the model tests on selected surfaces.

Keywords: light scattering, modeling.

## 1. Introduction

The application of light scattering methods to the rough surface assessment is based on an electromagnetic field analysis of the light wave scattered by a rough surface [1], [2]. Two basic problems are distinguished in the scatterometry of the rough surface – the direct and inverse ones [3]. They are presented schematically in Fig. 1. The direct problem consists in searching for the distribution of the electromagnetic field of the light wave scattered by the rough surface if the function describing the surface roughness  $z = f(x_s, y_s)$  is known and if we know the way of its illumination. The inverse problem consists in determination of the function describing the surface roughness  $z = f(x_s, y_s)$  from the measured intensity distribution  $I(x_p, y_p)$  of the light wave scattered by the rough surface.

In work [4], a solution to the inverse problem, which makes it possible to retrieve surface roughness by measuring the scattered field, was proposed. However, experimental investigations into the correctness of the proposed method of solving the inverse problem and the results obtained could be quite complicated. Numerical model tests seem to be much simpler. Therefore, the method and the results of the inverse problem modeling are presented briefly in further part of the paper. To verify the

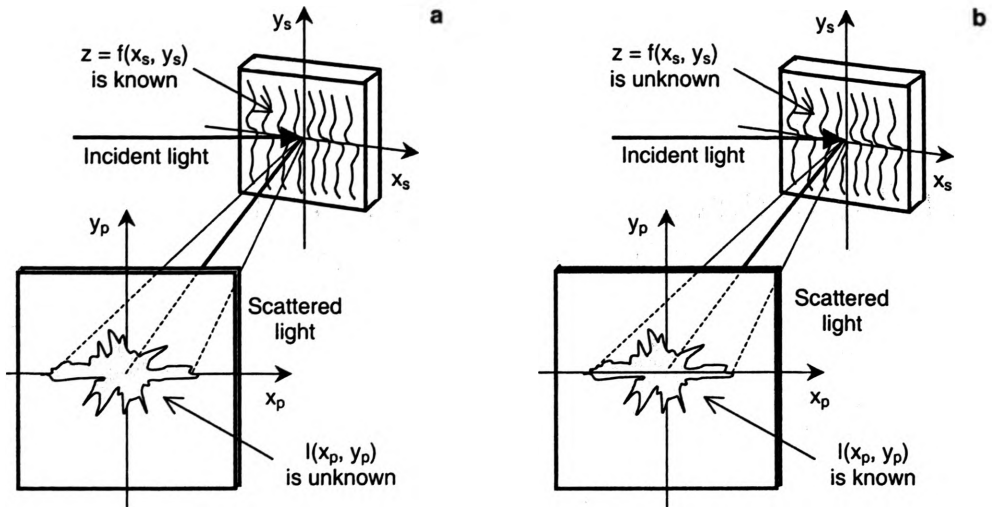


Fig. 1. Schematic representation of the direct problem (a), and of the inverse problem (b).

correctness of the assumed model of light scattering by a rough surface, the direct problem modeling preceded the modeling of the inverse problem.

Approaching the modeling of the direct and inverse problems a series of assumptions were made. First of all, it was assumed that the phenomenon of light scattering is described precisely enough in form of the scalar Kirchhoff theory of diffraction [5], [6]. Another assumption was that the surface of an object reflects the plane wave of monochromatic light with wavelength  $\lambda$  striking on the surface at normal incidence. A paraxial approximation was also made. We also assumed that the scattering surface is situated in the primary focal plane of the lens with equal focal lengths. The scattered field with the application of Fraunhofer approximation was analyzed in the secondary focal plane of this lens. These assumptions made it possible to use Fourier transformation in the process of modeling the diffraction field distributions. Furthermore, the intensity of light striking on the surface and the value of the amplitude reflection coefficient were taken to be equal to 1.

## 2. Modeling of direct problem

Model tests on the direct problem were carried out using the special software. This software was developed in two options. One of them was designed for modeling the phenomenon of light diffraction on two-dimensional (2D) rough surfaces  $z = f(x_s)$ , whereas the other – on three-dimensional (3D) rough surfaces  $z = f(x_s, y_s)$ . Both software options made it possible to set the function determining the height of irregularities at individual points of the surface, and determine the complex light amplitude  $E(x_s, y_s)$  at those points according to the following equation:

$$E(x_s, y_s) = \exp\left[i \frac{4\pi}{\lambda} f(x_s, y_s)\right] \tag{1}$$

where  $i$  is the imaginary unit,  $\lambda$  – the wavelength of light, and  $f(x_s, y_s)$  – the function describing the height of surface irregularities.

The next stage of modeling included Fourier transformation of the complex light amplitude on the surface by means of the fast Fourier transform. Then the squared modulus of Fourier transform was calculated

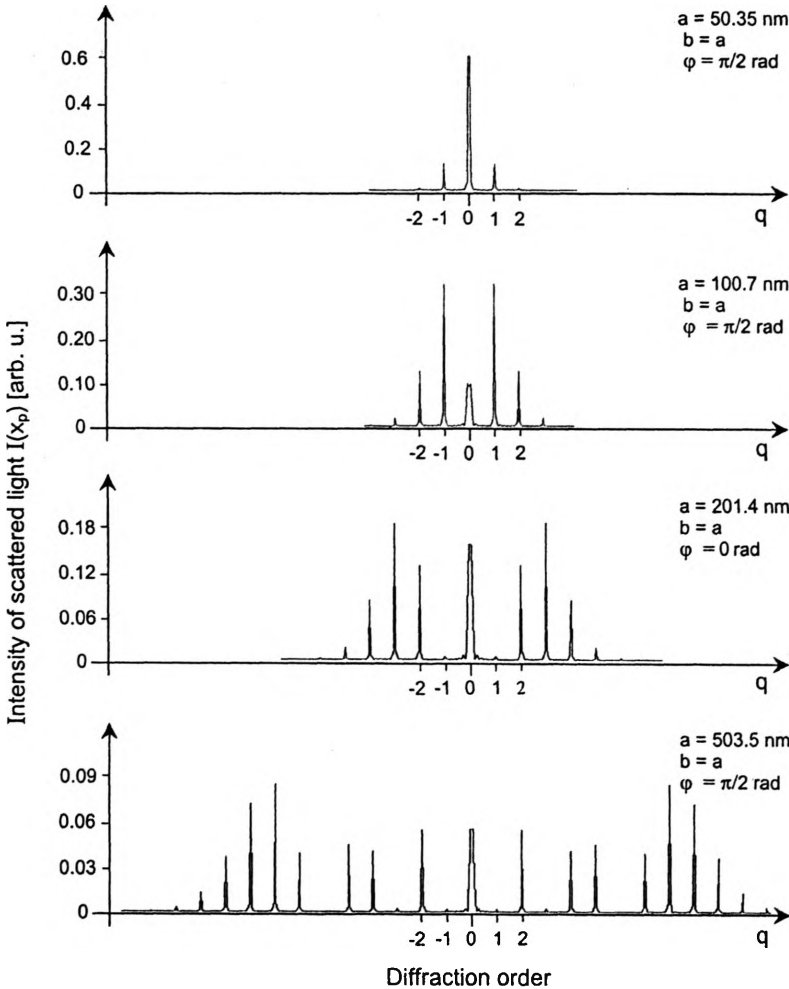


Fig. 2. Modeled distributions of the light intensity in Fraunhofer zone for scattered light from sinusoidal surface  $z = b + a\sin(x_s + \varphi)$ ; light wavelength  $\lambda = 632.8 \text{ nm}$ .

$$I(x_p, y_p) = |E(x_p, y_p)|^2 = \frac{1}{(\lambda f)^2} |\mathfrak{F}[E(x_s, y_s)]|^2 \tag{2}$$

where  $I(x_p, y_p)$  and  $E(x_p, y_p)$  are the intensity and the complex light amplitude in the secondary focal plane of the lens, respectively,  $\lambda$  is the wavelength,  $f$  – the lens focal length, the symbol  $\mathfrak{F}$  stands for Fourier transformation, and  $E(x_s, y_s)$  is the complex amplitude on the scattering surface.

Diffraction fields of the plane wave of coherent light in Fraunhofer zone were modeled for 2D and 3D surfaces. Periodic and aperiodic surfaces were tested. The plots of the light intensity obtained for the sinusoidal surfaces with different amplitudes are presented in Fig. 2. The normalized values of the light intensity are shown on vertical axes. Numbers of consecutive diffraction maxima are marked on horizontal axes. Comparing these results with the results presented by GOODMAN [5] and

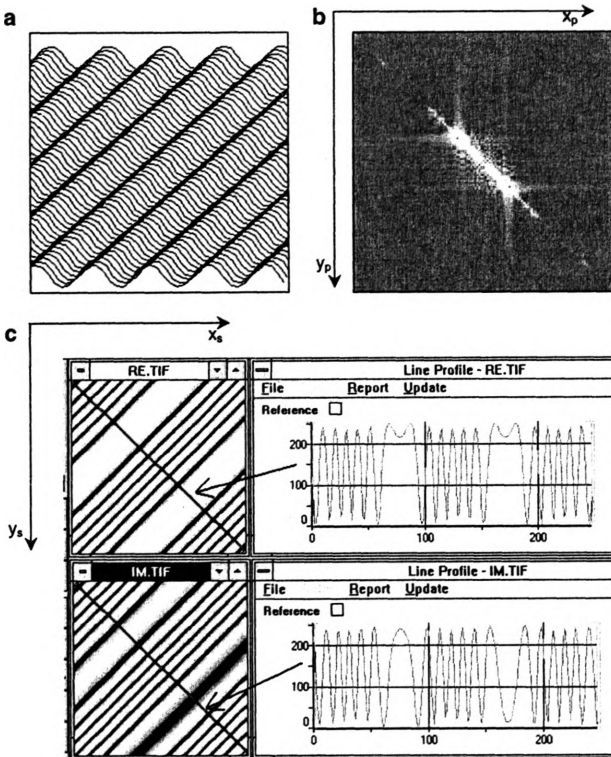


Fig. 3. Results of computer modeling of diffraction field scattered from sinusoidal surface  $z = a \sin[2\pi f_{xy}(x_s + y_s) + \varphi]$  in Fraunhofer zone, for amplitude  $a = 1 \mu\text{m}$ , spatial frequency  $f_{xy} = 20 \text{ mm}^{-1}$ , phase  $\varphi = 3 \text{ rad}$  and light wavelength  $\lambda = 632.8 \text{ nm}$ . Isometric plot of the scattering surface (a), intensity distribution of the scattered light  $I(x_p, y_p) \propto |\mathfrak{F}[E(x_s, y_s)]|^2$  in Fraunhofer zone (b), images of real and imaginary parts of the complex amplitude  $E(x_s, y_s)$  on sinusoidal surface and plots of both the parts obtained for  $x_s = y_s$  (c).

CATHEY [7], obtained for the diffraction of light transmitted through the sinusoidal grating, is indicative of the correctly developed algorithm of modeling.

Model tests of the direct problem on 3D surfaces were carried out over the illuminated area of  $256 \times 256$  pixels. Sample results of the modeling are illustrated in Fig. 3. The diffraction field in Fraunhofer zone was obtained for the sinusoidal surface with amplitude equal to  $1 \mu\text{m}$  and spatial wavelength of  $50 \mu\text{m}$ . In the course of the modeling calculations were made on 32-bit gray-level images. Figure 3a illustrates the shape of scattering surface, while Fig. 3b shows the calculated distribution of the intensity of light scattered by that surface.

The plots of the imaginary and real parts of complex amplitude  $E(x_s, y_s)$  on the sinusoidal surface are shown in Fig. 3c. They are traced along the line for which  $x_s = y_s$ . One can observe that these plots are similar to typical interferograms obtained during the harmonic motion of the interferometer mirror. This was already predicted in [8], where a laser interferometer was proposed to use for modeling the phenomenon of light scattering by rough surfaces.

It is clearly seen from Fig. 3c that the amplitude of functions  $\text{Re } E(x_s, y_s)$  and  $\text{Im } E(x_s, y_s)$  in the area of increased signal frequency is not constant. This is caused mainly by a comparatively small spatial resolution of the function being modeled. It reduced the range of amplitudes and spatial frequencies of modeled functions and the accuracy of results obtained. It is necessary to apply a higher spatial resolution in order to obtain better results of modeling of the direct and inverse problems on 3D surfaces. Therefore, the inverse problem has been modeled mainly on 2D surfaces.

### 3. Modeling of inverse problem

Model tests of the inverse problem were carried out on 2D surfaces  $z = f(x_s)$  using specially designed computer software. It was possible, at consecutive stages, to generate the surface profile, modify the complex light amplitude and then reproduce the irregularity profile according to methods described in [4].

Assumptions made for model tests were similar to those for modeling the direct problem. The algorithm applied to the process of modeling of the inverse problem described to a greater extent in work [4] covered the following procedures:

- generation of the odd function  $z = f(x_s)$  describing the surface,
- determination of the complex amplitude  $E_H(x_s)$  on the surface (Hermitian function),
- introduction of the unit pulse to the origin of coordinates,
- calculation of the attenuating function and the complex amplitude  $E_N(x_s)$  after modification,
- calculation of the scattered light intensity in Fraunhofer zone  $I(x_p)$ ,
- determination of the even and odd parts of the complex amplitude  $E(x_p)$ ,
- inverse Fourier transformation of the even and odd parts of  $E(x_p)$ ,

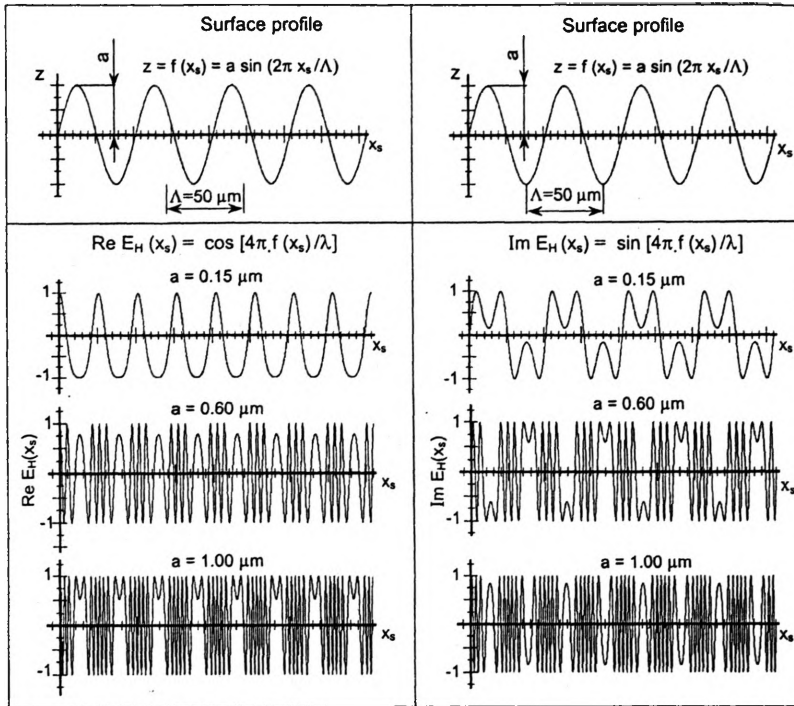


Fig. 4. Plots of real and imaginary parts of the complex amplitude  $E_H(x_s)$  on sinusoidal surface obtained for several values of amplitude  $a$ .

- removal of the unit pulse and amplification of the complex amplitude  $E_N(x_s)$ ,
- reconstruction of the function  $z = f(x_s)$  from the retrieval complex amplitude  $E_H(x_s)$ .

Model tests of the inverse problem were carried out for a series of selected periodic profiles with amplitudes not exceeding  $1 \mu\text{m}$ . In the case of a sinusoidal profile, like for other odd functions, the complex light amplitude  $E_H(x_s)$  is Hermitian function. Figure 4 includes the plots of the real and imaginary parts of the complex amplitude  $E_H(x_s)$  for modeled sinusoidal profiles with different amplitudes  $a$ . One can notice that an increase of the profile amplitude causes an increase in the spatial frequencies of the complex amplitude  $E_H(x_s)$ .

To analyze the effects of additional modification of the function  $E_H(x_s)$  on its amplitude spectrum, this spectrum was modeled before and after modification of the complex amplitude  $E_H(x_s)$ . Figure 5 illustrates sample plots obtained at successive stages of modeling. The coordinate system was selected so as to determine the diffraction order  $q$  on the horizontal axis. These plots were determined for the sinusoidal surface, shown in Fig. 4, with the amplitude  $a$  equal to  $0.15 \mu\text{m}$ .

The real part of Fourier transform of the complex amplitude  $E_H(x_s)$  before its modification is shown in Fig. 5a. It is obvious that the imaginary part of this transform is equal to zero. It results from Fig. 5a that Fourier transform of the complex amplitude  $E_H(x_s)$  includes harmonics with different signs.

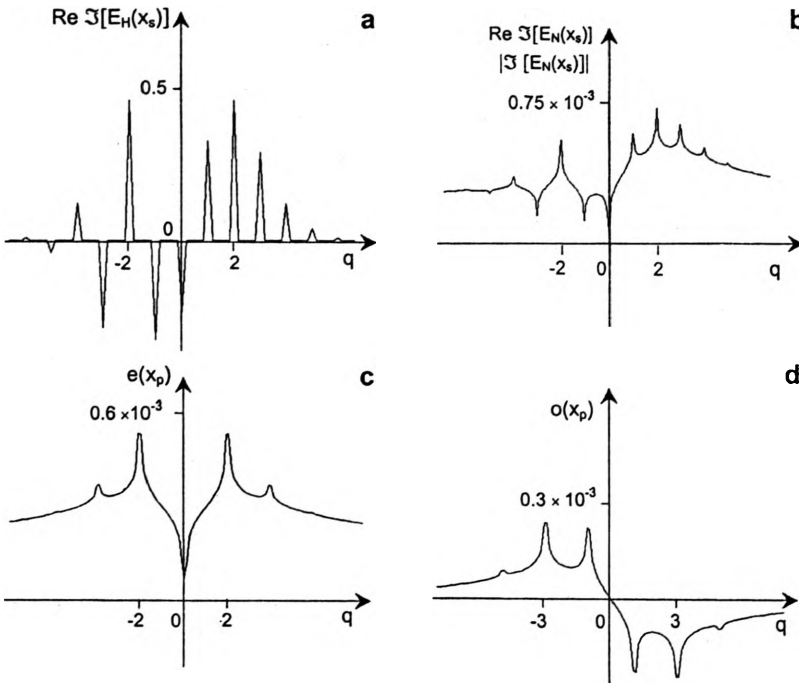


Fig. 5. Plots obtained during modeling of Fourier transform of the complex amplitudes  $E_H(x_s)$  and  $E_N(x_s)$  on sinusoidal surface shown in Fig. 4, for amplitude  $a = 0.15 \mu\text{m}$ . Plot of real part of  $\Im[E_H(x_s)]$  (a), plot of real part of  $\Im[E_N(x_s)]$  (b), plot of even part of  $\Im[E_N(x_s)]$  (c), plot of odd part of  $\Im[E_N(x_s)]$  (d).

The plot obtained by modeling Fourier transform of the complex amplitude  $E_N(x_s)$  is presented in Fig. 5b. The procedure for determination of the complex amplitude  $E_N(x_s)$  is included in work [4]. Successive modification stages of the function  $E_H(x_s)$ , allowing the complex amplitude  $E_N(x_s)$  to be obtained, are presented there. According to Fig. 5b all the values of Fourier transform of the complex amplitude  $E_N(x_s)$  are positive and equal to its modulus. Nevertheless, these values are about 1000 times lower than values of Fourier transform of the function  $E_H(x_s)$ . This is affected by attenuation of the function  $E_H(x_s)$  during its modification. Such a reduction of measuring signals during the profile reconstruction based on measurements of the diffraction field is disadvantageous. In practice, it can be partly compensated for by applying light sources with increased power to illuminate the surface.

In the course of model tests the even part  $e(x_p)$  and the odd part  $o(x_p)$  of Fourier transform of the complex amplitude  $E_N(x_s)$  were determined as well. Both the parts were calculated making use of the light intensity values obtained by modeling. Figure 5c and d show the plots of the even and odd parts of Fourier transform of the function  $E_N(x_s)$ . These plots, like previously, apply to the sinusoidal surface with the amplitude  $a = 0.15 \mu\text{m}$ .

At the next stage of modeling the inverse problem the light phase was retrieved on the rough surface. Therefore, the inverse Fourier transformation of the even part  $e(x_p)$

and the odd part  $o(x_p)$  of Fourier transform of the function  $E_N(x_s)$  was implemented. Then the transformations inverse to those which were performed during modification of the function  $E_H(x_s)$  were carried out. Owing to that, the real part and the imaginary part of the complex light amplitude  $E_H(x_s)$  were obtained on the rough surface.

The final stage of the inverse problem modeling was aimed to determine the surface profile  $z=f(x_s)$  based on the real and imaginary parts of the complex amplitude  $E_H(x_s)$ . At the same time, trigonometric functions, the arc sine and arc cosine, were applied. In every case, the model tests resulted in obtaining the correct profile of the surface  $z=f(x_s)$ .

## 4. Conclusions

The model tests proved that methods of solving the inverse problem proposed in [4] are correct. However, it should be taken into account that their implementation is not going to be easy regarding many conditions to be fulfilled. Application of these methods in practice should be preceded by further investigations. However, for the present one may say that these methods will be useful for assessment of periodic surfaces with small amplitudes. The proposed method of solving the inverse problem may also find application to more general problems where knowing the squared modulus of Fourier transform of the function with phase modulation one may aim at retrieving the information on the phase of this function.

## References

- [1] BENNETT J.M., MATTSSON L., *Introduction to Surface Roughness and Scattering*, Optical Society of America, Washington, D.C., 1989.
- [2] STOVER J.C., *Optical Scattering: Measurement and Analysis*, McGraw-Hill, Inc., New York 1990.
- [3] ŁUKIANOWICZ C., Proc. SPIE **4517** (2001), 120.
- [4] ŁUKIANOWICZ C., Opt. Appl. **33** (2003), 315.
- [5] GOODMAN J.W., *Introduction to Fourier Optics*, McGraw-Hill Book Co., London 1968.
- [6] OGILVY J.A., *Theory of Wave Scattering from Random Rough Surfaces*, Adam Hilger, Bristol, Philadelphia and New York 1991.
- [7] CATHEY W.T., *Optical Information Processing and Holography*, Wiley, New York 1974.
- [8] ŁUKIANOWICZ C., Precision Eng. **7** (1985), 67.

*Received July 11, 2002*